Synthesis and Characterization of Electropolymerized Poly(cyclophosphazene−benzoquinone)

Jing Li and Mira Josowicz*

Materials and Chemical Sciences Department, Pacific Northwest National Laboratory,† Richland, Washington 99352

Received March 3, 1997[⊗]

Formation of a inorganic−organic hybrid material from hexachlorocyclotriphosphazene, $(NPCl_2)_3$, and quinone precursors directly at the electrode surface was studied. These materials are formed from electrochemically generated quinone radical anion and quinone dianion at the electrode surface followed by nucleophilic substitution of the chlorine on the phosphazene heterocycle. The polymerization process is controlled by the electrochemical−chemical−electrochemical−chemical.. (ECEC..) mechanism and is independent of the concentration of the BQ in the solution. The chemical composition of the poly(cyclophosphazene-benzoquinone), PPBQ, material was examined by elemental analysis and the X-ray photoelectron spectroscopy. ^{31}P Nuclear magnetic resonance, Fourier transform infrared spectroscopy, and X-ray diffraction were used to characterize the chemical structure of the material. The results confirm that the PPBQ is formed by replacement of four chlorine atoms on one $(NPCl_2)_3$ precursor by four quinones which are linked directly to the phosphorus through their oxygens. The resulting material is amorphous, chemically inert, electrically nonconducting, nonflammable, and porous. The thickness of PPBQ and porosity of the PPBQ can be controlled electrochemically.

Introduction

The possibility to design a method for synthesis of inorganic−organic coating has emerged interest in manipulation of molecular interactions between benzoquinone and hexachlorocyclophosphazene, also known as phosphonitrilic chloride trimer, $(NPCl_2)_3$. It is expected that the produced hybrid material will exhibit properties different from a totally organic polymer, for example, be resistant to organic solvents, and heat- and flame-retardant.[1,2] The reactivity of the P−Cl bond at the phosphazene trimer allows an easy access to nucleophilic substitution reactions, in which chlorine atoms can be replaced by a wide variety of organic, organometallic, or inorganic substituents.[3] The classical approach to preparing a cyclophosphazene-based inorganic−organic material involves a molten-phase thermal polymerization[4] or polymerization in organic solvents[4−7] in the presence of a bifunctional phenol. However, these processes lead only to low molecular weight compounds because an extensive substitution of all the chlorine atoms in $(NPCl_2)_3$ by aromatic groups inhibits farther polymerization.[3,8] As the solution to this problem it was proposed to leave some of the chlorine atoms attached to the trimer. When more than two chlorine atoms on the phosphazene trimer are substituted by the $O-C_6H_4-O$ group, the polymer chains grow in three dimensions.[1]

The aim of this work was to explore the possibility of using an electrochemical approach for depositing inorganic−organic material in situ on a surface of a conducting substrate. The electrochemical synthesis is attractive, because the production of active intermediates is efficient, the product is clean, and deposition control on the desired substrate area is good. A drawback of this approach is that phosphazenes that contain the most electronegative ligands such as fluorine, chlorine, bromine, or trifluoroethoxy is not electrochemically active.[9] In this paper, we describe a solution to this problem, which involves formation of an intermediate adduct between the $(NPCl_2)_3$ precursor and an active form of a reactant. In the preliminary work it was found that the free radicals formed during electrochemical reduction of benzoquinone can act as active intermediates for $(NPCl_2)_3$ coupling leading to the formation of a polymeric cyclophosphazene−benzoquinone, PPBQ, material.[10] The coupling between the benzoquinone (BQ) intermediates and the $(NPCl_2)_3$ is a typical electrochemical−chemical (EC) reaction. Parameters that mainly affect the electrochemical synthesis of the hybrid material, such as water, oxygen and the cathodic potential, and different solvents, were optimized. The composition of the synthesized films was determined by elemental analysis and X-ray pho-

* To whom correspondence concerning this paper should be addressed.

† Pacific Northwest National Laboratory is operated by Battelle Memorial Institute for the U.S. Department of Energy under Contract No. DE-ACO6-76RLO#1830.

⊗ Abstract published in *Advance ACS Abstracts,* May 1, 1997.

(1) Mark, J. E.; Allcock, H. R.; West, R. *Inorganic Polymers*; Polymer Science and Engineering Series; Prentice Hall Inc.: Englewood Cliffs, NJ, 1992; p 61.

(2) Allcock, H. R.; Best, R. J. *Can. J. Chem.* **1964**, *42*, 447.

(3) Allcock, H. R. J. *Inorg. Organomet. Polym.* **1992**, *2*, 197.

(4) Yokoyama, M; Cho, H; Kono, K. *Kogyo Kagaku Zasshi* **1964**, *67*, 1378.

(5) Zhivukhim, S. M.; Kireev, V. V.; Zelenetskii, A. N. *Zh. Prikl. Khim.* **1966**, *39*, 234 (Russian).

(6) Zhivukhim, S. M.; Kireev, V. V.; Aulova, N. V.; Gerasimenko. D. I. *Dokl. Akad. Nauk SSSR* **1964**, *158*, 896 (Russian).

(7) Zhivukhim, S. M.; Totstguzov, V. B.; Kireev, V. V. *Plast. Massy* **1963**, *7*, 24.

(8) Allcock, H. R.; Dembek, A. A.; Mang, M. N.; Riding, G. H.; Parvez, M.; Visscher, K. B. *Inorg. Chem.* **1992**, *31*, 2734.

(9) Allcock, H. R.; Birdsal, W. J. *Inorg. Chem.* **1971**, *10*, 2495.

(10) Josowicz, M.; Li, Jing; Exarhos, G. J. *J. Electrochem. Soc.* **1994**, *141*, L162.

S0897-4756(97)00136-1 CCC: $14.00

toelectron spectroscopy (XPS). The structure of the material was identified by the Fourier transform infrared spectroscopy (FTIR) and by the ^{31}P nuclear magnetic resonance (NMR). The morphology of the material was investigated by X-ray diffraction, atomic force microscopy (AFM), and profilometry.

Experimental Section

Reagents. All chemicals were purchased from the Aldrich Chemical Co, Milwaukee. Hexachlorocyclotriphosphazene, $(NPCl_2)_3$ (99%), and 1,4-benzoquinone (BQ), or anthraquinone, 1,4 naphthoquinone , 1,5-dihydroxyanthraquinone (anthrarufin), were used as precursors as received. Tetrabutylammonium tetrafluoroborate (Bu_4NBF_4) (99%), was used as a supporting electrolyte after recrystallization from methanol (HPLC grade) and drying in the oven at 70 °C overnight. All other electrolyte salts, such as tetrabutylammonium iodide (Bu_4NI) (99%), and tetrabutylammonium tetraphenylborate (Bu_4NBPh_4) (99%), were used without further purification. Acetonitrile (CH_3CN) (anhydrous, 99+%) was kept under nitrogen. The water content in CH_3CN was less than 0.005 vol %. The tetrahydrofuran (THF), dimethyl sulfoxide (DMSO), and propylene carbonate were used as received. Silver nitrate ($AgNO_3$, 99+%) was the electrolyte salt for the Ag/0.1 M Ag^+ reference electrode. *Caution: CH_3CN, THF, and DMSO are irritating to skin, eyes, and mucous membrane and they are flammable liquids.*

Synthesis of the PPBQ Coating. The experiments were carried out in either one- or three-compartment cells. An EG&G, Princeton Applied Research (PAR) Model 273 potentiostat−galvanostat, controlled by EG&G Electrochemical Analysis Software 3.00, was used in conjunction with a Northgate Computer (Northgate Computer System Inc.) interfaced through IEEE 488 interface of the HP 34401A multimeter. In all experiments a silver reference electrode, Ag/0.1 M $AgNO_3$ in CH_3CN in a liquid junction contact with 0.1 M Bu_4NBF_4 in CH_3CN, was used. In the one-compartment cell experiments, a platinum disk of 0.3 cm in diameter (A = 0.07 cm^2) (Bioanalytical Systems, Inc.) was used as a working electrode, and a large platinum foil (A = 37.5 cm^2) was used as the counter electrode. Besides the Pt working electrode also copper, lead, silver, titanium, tungsten, and indium−tin oxide (ITO) were used. In the three-compartment cell experiments, two compartments were used for the anolyte and one compartment for the catholyte. The compartments were separated by two glass ceramic disk frits. A platinum foil with a surface area of 0.6 cm^2 was used as a working electrode, and two square platinum foils with a surface area of 10 cm^2 each were placed as counter electrodes in each anolyte compartments. The substrates were hand polished with 1 μm aluminum powder (Buhler) and rinsed several times with water and then with acetonitrile before every use.

The films were deposited on the working electrode by potentiostatic or by galvanostatic techniques, respectively. All film depositions were done in acetonitrile solution containing 0.01 M BQ and 0.1 M Bu_4NBF_4 in the presence of 0.01 M $(PNCl_2)_3$. The 10 mM concentration of $(NPCl_2)_3$ was set in accordance with its highest solubility in acetonitrile. The potential of the working electrode was applied from the open cell potential of −0.24 V up to −1.0 or −2.0 V. However, any potential between −1.0 and −2.0 V on the reductive side was also found to be satisfactory. The thickness of the deposited coating was controlled by the number of applied potentiostatic cycles or by deposition time. The thickness of the PPBQ film correlates linearly with the charge used for the film synthesis.

General Physical and Chemical Characterization Methods. Ultraviolet/visible (UV/vis) absorption spectra of BQ in acetonitrile solution were measured before and after electrolysis carried out in a three-compartment cell. The spectra were obtained on a Varian Cary 5 UV−vis−near-IR spectrophotometer using Varian Cary OS/2 multitasking software. The UV/vis absorption spectra of the solution were measured from 200 to 780 nm at a scan rate of 1000 nm/min. Quartz cuvettes (Helma) of 0.2 cm path length (1 cm^3) were used. The spectrum of BQ in acetonitrile was not influenced by the presence of 0.1 M Bu_4NBF_4 and 0.01 M $(NPCl_2)_3$. Samples of electrolytes were obtained from the catholyte compartment of the three-compartment cell. The samples were diluted 1:20 with acetonitrile before the optical spectra were recorded.

Elemental analyses experiments were done by the Schwarzkopf Microanalytical Laboratory, New York. The deposited PPBQ films on platinum foil were washed several times with acetonitrile and then with deionized water and finally dried with nitrogen. The analyses were done on powder samples that were obtained by scratching off the coating from the Pt foil used as the electrode. Elemental analysis for phosphorus, nitrogen, carbon, hydrogen, chlorine, and fluorine or iodine was performed on 17 mg samples. The amount of oxygen was assumed to be the difference between 100% and the total of the other measured elements.

X-ray photoelectron spectroscopy (XPS) surface compositional studies were performed with a Physical Electronics Model 560 spectrometer with a double-pass cylindrical mirror analyzer (Mg Kα line at $h\nu$ = 1253.6 eV). The survey scans (0−1000 eV binding energy) were recorded with a pass energy of 100 eV. The absolute energy scale and linearity of the analyzer were calibrated to Cu 3p at 75.14 ± 0.03 and Cu $2p_{3/2}$ at 932.66 ± 0.03. The residual pressure in the spectrometer was approximately 10^{-8} Torr during the data acquisition. The binding energies for identical samples were, in general, reproducible to within ±0.1 eV. The XPS data were obtained on PPBQ films deposited on a platinum foil.

Fourier transform infrared (FTIR) spectroscopic studies were done on hexachlorocyclophosphazene, benzoquinone, and hydroquinone dispersed in KBr disks with a Nicolet 740 FTIR spectrometer. The instrument was purged with dry nitrogen and equipped with liquid-nitrogen cooled (wide band) mercury cadmium telluride detector during collection of IR spectra. All IR spectra were collected between 400 and 4000 cm^{-1} and were baseline corrected. The spectra were acquired by signal averaging of 64 scans at a normal resolution of 4 cm^{-1} with Nicolet's 660 data system and plotted on the HP 7470A plotter. Attenuated total reflectance infrared (ATR-IR) spectroscopic measurements were performed on PPBQ films deposited onto 300 Å Au/glass substrates placed in contact with the ZnSe crystal element of the ATR attachment.

^{31}P NMR spectroscopy studies were done with a Brucker ACF 300 FT-NMR spectrometer. The solid phosphorus ^{31}P NMR (4.7 kHz) spectrum of PPBQ polymer was recorded. A broadband (cross-polarization via spinock with bilevel decoupling) probe (7 mm in diameter) was used. The ^{31}P chemical shifts were referenced to solid triphenylphosphine, $(C_6H_5O)_3P$, at δ = −3.1 ppm for phosphorus, which corresponds to 85% H_3PO_4 at standard (0 ppm).

Thickness and roughness measurements of the deposited coatings were carried out with a Dektak 8000 Surface Profile Measuring System from Veeco, Sloan Technology, Inc. The coatings were scanned with a 12 μm stylus with a 1 mg force at a medium rate of 13 s per scan.

Optical microscopy investigations were carried out with a digital confocal microscope, Nikon, Inc. The PPBQ images were acquired using Volscan 2 and Micro-Tome II (Vay Tek, Inc.) software.

X-ray diffraction studies of the powdered form of PPBQ coating were carried out with a Philips X-ray diffractometer (M&TE ID#APD3620). The X-ray source was a rotating anode with a copper target and graphite monochromated radiation. Data were collected between 5° and 50° in 2θ range with a step size of 0.05° and a count time 60 s/step. A very slow scan rate of 0.05°/60 s was applied for the whole 2θ range of 5° to 50°. The sample was used as the cathode.

The density of the PPBQ was determined by the dual quartz crystal microbalance.[11] The films were electrochemically deposited in the following two ways: (1) The potential was

(11) Dunham, G.; Benson, N. H.; Petelenz, D.; Janata, J. *Anal. Chem.* **1993**, *67*, 267.

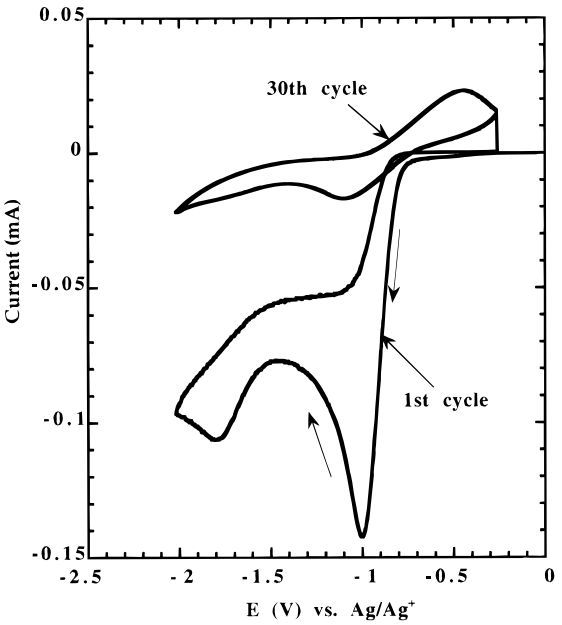

Figure 1. Cyclic voltammogram of 10 mM BQ recorded on platinum electrode in the presence of 10 mM $(NPCl_2)_3$ with 0.1 M Bu_4NBF_4 in acetonitrile from −0.2 to −2.0 V with sweep rate of 100 mV/s. The first and last cycles are shown.

cycled from −0.2 to −2 V for 15 min with scan rate of 100 mV/s. The thickness of the PPBQ film was measured to be 2.3 μm. The weight was 298.152 mg/cm^2. The density was calculated to be 1.295 g/cm^3. (2) A constant potential of −2 V was applied for 10 min. The PPBQ film was 1 μm thick and weight 121.7 mg/cm^2. The density calculated for this film was 1.217 g/cm^3.

An electrothermal melting point apparatus was used to determine the melting point of PPBQ. As the white powder sample was heated from room temperature up, at 240 °C the sample became gray and started to sublime. That indicated some thermal decomposition of the sample.

Results and Discussion

Polymer Synthesis. The cyclic voltammograms of the supporting electrolyte, 0.1 M Bu_4NBF_4 on its own or in the presence of 0.01 M $(NPCl_2)_3$ precursor, do not display any electrochemical activity within the examined electrochemical window from +2 to −2 V.[9,10,14,15] The use of Bu_4NBF_4 does not affect the redox chemistry of the BQ in acetonitrile.[10,16] However, an addition of 0.01 M BQ to the solution of 0.01 M $(NPCl_2)_3$ and 0.1 M Bu_4NBF_4 in acetonitrile and repetitive cycling of the potential of the working electrode between −0.24 and −2 V leads to electrochemical reaction and deposition of a white coating on the cathode. Figure 1 shows the corresponding multisweep cyclic voltammogram. The poly(cyclophosphazene−benzoquinone), PPBQ coating also forms when the applied cathodic potential is limited to −1.2 V.[10] The use of organic solvents other than acetonitrile, such as propylene carbonate, tetrahydrofuran, or dimethyl sulfoxide, was limited by the low solubility of $(NPCl_2)_3$, and by their low decomposition potential on the reduction side.[12] Furthermore, it was observed that the thickness and roughness of the PPBQ films were influenced by the electrolyte salt. For example, PPBQ films deposited from Bu_4NI and Bu_4NBF_4 were of the same thickness but thicker than those deposited from Bu_4NBPh_4.

Other quinones besides the BQ, such as naphthoquinone, anthraquinone, and anthrarufin, can also form an intermediate which can react chemically with $(NPCl_2)_3$. The deposition was done at a constant potential of −2 V for 5 min on Pt electrode in the electrolyte solution containing always 0.1 M Bu_4NBF_4 and 0.01 M $(NPCl_2)_3$ and 0.01 M of naphthoquinone, anthraquinone, or anthrarufin, respectively. The micrographs of the deposited films are shown in Figure 2. The films have different morphology, which we believe is governed by the type of the quinone molecule. In further studies we have concentrated only on the copolymerization reaction of BQ with $(PNCl_2)_3$.

We observed that the thickness of the deposited PPBQ layer and the morphology of the film depend on the magnitude of the applied potential and on the way how it was applied (step or sweep), but it does not depend on the concentration of BQ in solution. For example, coatings grown by applying a potential step from −0.2 to −2 V for 5 min were approximately 4 μm thick with a roughness of ±0.5 μm. Films grown by sweeping the potential within the same rage (−0.2 and −2 V) for the same time were approximately 3.3 μm thick with a roughness of ±0.15 μm. For the PPBQ films grown between −0.25 and −1.0 V, the difference in thickness and roughness was comparable. Because the growth occurs cathodically, PPBQ coatings can be also obtained on copper, silver, titanium, tungsten, and indium/tin oxide (ITO) substrates.

In principle, the efficiency of the polymerization process can be affected by the presence of water (W) or oxygen (G) and by the voltage (U). The method of factorial analysis[12] was used to analyze the effects resulting of three interactions between two variables (WU), (UG), and (GW) and one interaction among all three (UGW). These effects were investigated at two different levels: with addition of 5 vol % water or without added water, with or without oxygen, and at constant cathodic potential applied from −0.24 to −1 or −2 V. The influence of water on the polymerization is determined by the hydrolysis of $(NPCl_2)_3$.[16] When the water concentration exceeded 5 vol % in the solution of 0.01 M $(NPCl_2)_3$ in CH_3CN the polymerization of PPBQ was not possible. In electrolyte solution with water contents below 5 vol %, polymerization of PPBQ was taking place but the polymerization efficiency was low because of protonation of BQ intermediates and hydrolysis of the Cl on the $(NPCl_2)_3$. Since the P−OH bond is less polarized than the P−Cl bond, even a partial hydrolysis of the $(NPCl_2)_3$ precursor significantly limits the number of the remaining chlorines. The factorial analysis results are summarized in Table 1. The analysis shows that the increase of the potential from −1 to −2 V and the absence of water and oxygen in the electrolyte make the synthesis of PPBQ film very efficient. This can be attributed to the presence of a high concentration of BQ intermediates formed at that electrode potential and to the rapid reaction with $(NPCl_2)_3$. The high yield of polymerization dropped by approximately 80% when the reaction was carried out at the same high potential, in the presence of oxygen

(12) Li, Jing, Ph.D. Thesis, University of Utah, 1996.
(13) Pinson, J.; Saveant, J.-M. *J. Am. Chem. Soc.* **1978**, *100*, 1500.
(14) Swartz, J. E.; Stenzel, T. T. *J. Am. Chem. Soc.* **1984**, *106*, 2520.
(15) Peover, M. E.; Davies, J. D. *J. Electroanal. Chem.* **1963**, *6*, 46.
(16) Allen, C. W. *The Chemistry of Organic Homo- and Heterocycles*; Academic Press Inc.: New York, 1987; Vol. 2, p 544.

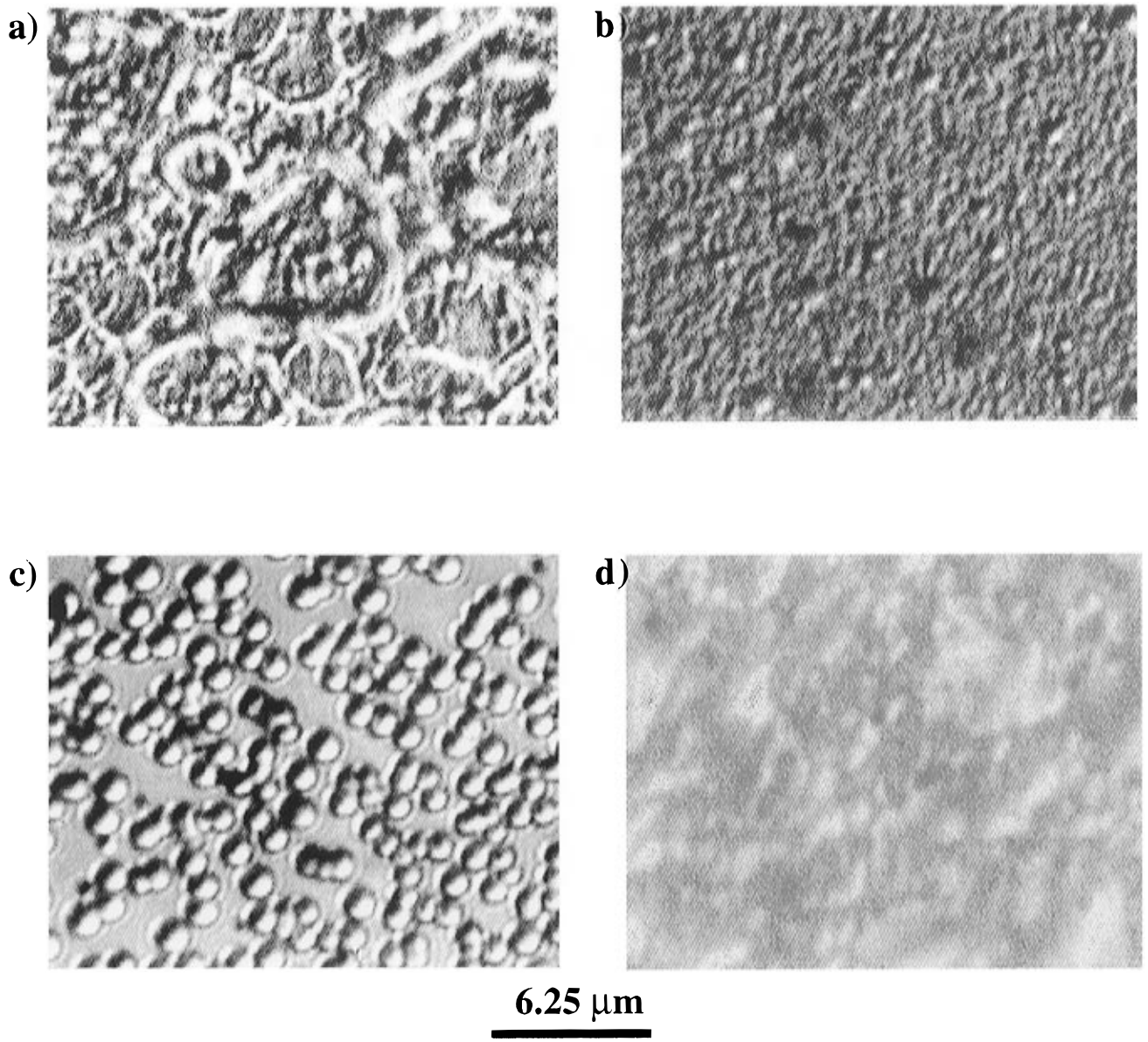

Figure 2. Optical micrographs of coatings obtained on Pt substrate during copolymerization of $(NPCl_2)_3$ with (a) benzoquinone, (b) naphthoquinone, (c) anthraquinone, and (d) anthrarufin. All micrographs were taken with the same magnification.

Table 1. 2^3 Factorial Analysis of the Design and Yield of the Polymerization Process in Scope on the Thickness of the PPBQ Coatings (Ref 12)[a]

U = const		gas		water		
−1 V	−2 V	air	N_2	no	5 vol %	yield thickness, Å
x		x		x		3800
	x	x		x		2500
x			x	x		4200
	x		x	x		15300
x		x			x	2600
	x	x			x	2400
x			x		x	3000
	x		x		x	3200

[a] The PPBQ films were deposited at constant potential.

but in the absence of water. That profound inhibition of PPBQ polymerization is believed to be driven by a recombination step of the BQ intermediates formed at the electrode surface. A similar pattern but much less crucial has been observed when the PPBQ polymerization was carried out at −1 V.

Mechanism of PPBQ Electrodeposition. To evaluate the reactivity of the BQ intermediates, a closer examination of the electrochemical reduction of 0.01 M BQ in CH_3CN acetonitrile was necessary. It is known that under aprotic conditions quinones undergo two one-electron reduction steps:[17−19]

$$BQ + e \Leftrightarrow BQ^{\bullet -} \quad (1)$$

$$BQ^{\bullet -} + e \Leftrightarrow BQ^{2-} \quad (2)$$

In agreement with potentiostatic experimental conditions at $t = 0$, only the BQ species are present in the bulk of the solution, whereas the concentration of benzoquinone radical anion, $BQ^{\bullet -}$, and benzoquinone bianion, BQ^{2-}, are zero. When a cathodic potential sweep is applied to the working electrode, two reduction waves appear (Figure 3). The first wave at, $E_{pc1} = -0.86$ V corresponds to the formation of $BQ^{\bullet -}$ and the second wave, $E_{pc2} = -1.495$ V, corresponds to the formation of

(17) Given, P. H.; Peover, M. E. *Trans. Faraday. Soc.* **1962**, *58*, 1656.
(18) Brown, A. P.; Anson, F. C. *Anal. Chem.* **1977**, *49*, 1589.
(19) Given, P. H.; Peover, M. E.; Schoen, J. *J. Chem. Soc.* **1958**, 2674.

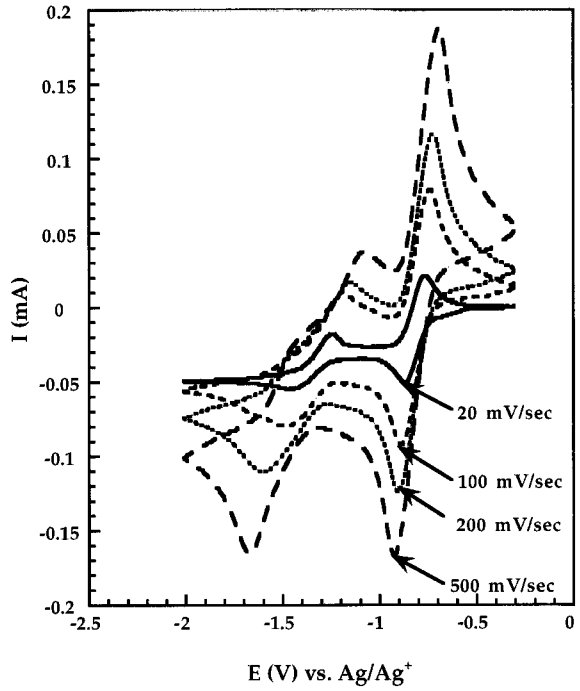

Figure 3. Cyclic voltammograms of 10 mM benzoquinone recorded on platinum electrode in the presence of 0.1 M Bu_4NBF_4 in acetonitrile from −0.2 to −2.0 V, at different scan rates.

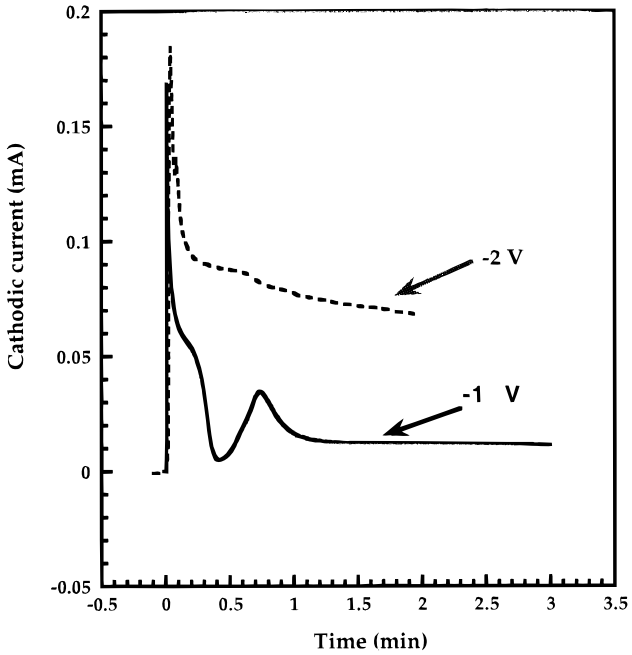

Figure 4. Comparison of PPBQ synthesis carried out at constant potential of −1.0 and −2.0 V on platinum electrode in a solution as described for Figure 1.

BQ^{2-}. In agreement with eqs 1 and 2 the electroactive species formed at E_{pc1} and E_{pc2} respectively, result from two separate charge-transfer reactions. In comparison with the E_{pc1} wave, the peak current of the E_{pc2} wave is always lower and the reduction waves are always drawn out with increasing sweep rates. When the potential is limited to −1.2 V, the separation of the cathodic and anodic peak potentials is well-defined.[10] Cyclic voltammogram responses obtained at scan rates below 0.1 V/s indicate that the height of the peak current (i_p) is linearly proportional to the square root of the sweep rate ($\nu^{1/2}$) and the ratio of the cathodic and anodic peak currents equals one. For the initial concentration of 10 mM BQ, the diffusion constant for BQ species was calculated to be $D = 3.7 \times 10^{-6}$ cm/s.[12] Using the Randles−Sevcik equation, $i_p = (2.69 \times 10^5)\, n^3 A D^{1/2} \nu^{1/2} C$, the number ($n$) of electrons involved in the first cathodic charge-transfer reaction, eq 1, was calculated to be 0.95. This is in close agreement with the reversible one-electron process described in the literature.[22,23] This means that there is no follow-up chemical reaction after the initial electron-transfer reaction.[21,22] As seen in Figure 3, sweep rates greater than 0.1 V/s were causing shifts in the position for both of the oxidation and reduction peak potentials, and an increase of the cathodic peak current and broadening of the redox peaks. The ratio of the linear sweep constant ($i_p \nu^{-1/2}$) to the potential step rate ($i_d t^{1/2}$) of the first reduction wave is not linear for the faster scan rates.[12] This result means that under these conditions, the redox system given by eq 1, is limited by kinetic process. Indeed, applying the equation for irreversible electron transport, for which the peak potential is given by $E_p = E_{1/2} - b[0.52 - 0.5 \log(b/D) - \log k_s + 0.5 \log n]$, the $b/2$ values were obtained.[25] Using data points presented in Figure 3, plots of E_p vs log ν for oxidation and reduction processes were made and the slopes b determined.[12] The specific rate constant k_s for the first redox reaction (eq 1) was calculated to be for the reduction, $k_1 = 1.2 \times 10^{-4}$ cm/s and for the reoxidation, $k_{-1} = 2.4 \times 10^{-4}$ cm/s. Assuming that the diffusion coefficient of the BQ^{2-} and $BQ^{\bullet -}$ are approximately the same, we obtained for the second redox reaction (eq 2), $k_2 = 7.2 \times 10^{-5}$ cm/s and $k_{-2} = 1.4 \times 10^{-4}$ cm/s, respectively. Because $k_1 < k_{-1}$ and $k_2 < k_{-2}$, the $BQ^{\bullet -}$ or/and BQ^{2-} are accumulated in the reaction zone in front of the electrode to form the polymer. Furthermore, when $k_{-2} < k_{-1}$ the reoxidation wave is shifted to more anodic potential values than the standard redox potential eq 2 . An increase of scan rates (Figure 3) increases the peak separation between the redox potentials and decreases the ratio of i_{pc}/i_{pa}. This indicates that, besides the homogeneous charge transfer leading to the formation of $BQ^{\bullet -}$ at the electrode surface, some heterogeneous follow-up reactions are taking place.[26] The basic $BQ^{\bullet -}$ is easily protonated even by weak proton donors, such as water, to form *p*-benzohydroquinone radical, $BQH^{\bullet}$:

$$BQ^{\bullet -} + H^+ \leftrightarrow BQH^{\bullet} \quad (3)$$

$$BQH^{\bullet} + e \leftrightarrow BQH^- \quad (4)$$

The reduction potential of $BQH^{\bullet}$ is more positive than that of $BQ^{\bullet -}$.[17] The electrochemical formation of $BQ^{\bullet -}$, its protonation to $BQH^{\bullet}$, and its electrochemical reduction to BQH^- drive the reactions in agreement with the

(20) Parker V. D. *Electroanalytical Chemistry*; Bard, A. J., Ed.; Dekker: New York, 1966; Vol. 14, p 1.
(21) Bard, A. J.; Faulkner, L. R. *Electrochemical Methods*; Wiley, New York, 1980.
(22) Pekmez, K.; Can, M.; Yildiz, A. *Electrochim. Acta* **1993**, *36*, 607.
(23) Eggins, B. R. *Chem. Commun.* **1969**, 1267.
(24) Fry, A. J. *Synthetic Organic Chemistry*; John Wiley & Sons: New York, 1989.
(25) Gileadi, E.; Kirova-Eisner, E.; Penciner, J. *Interfacial Electrochemistry*; Addison-Wesley Publ: New York, 1975; p 373.
(26) Laviron, E. *J. Electroanal. Chem.* **1983**, *38*, 1.

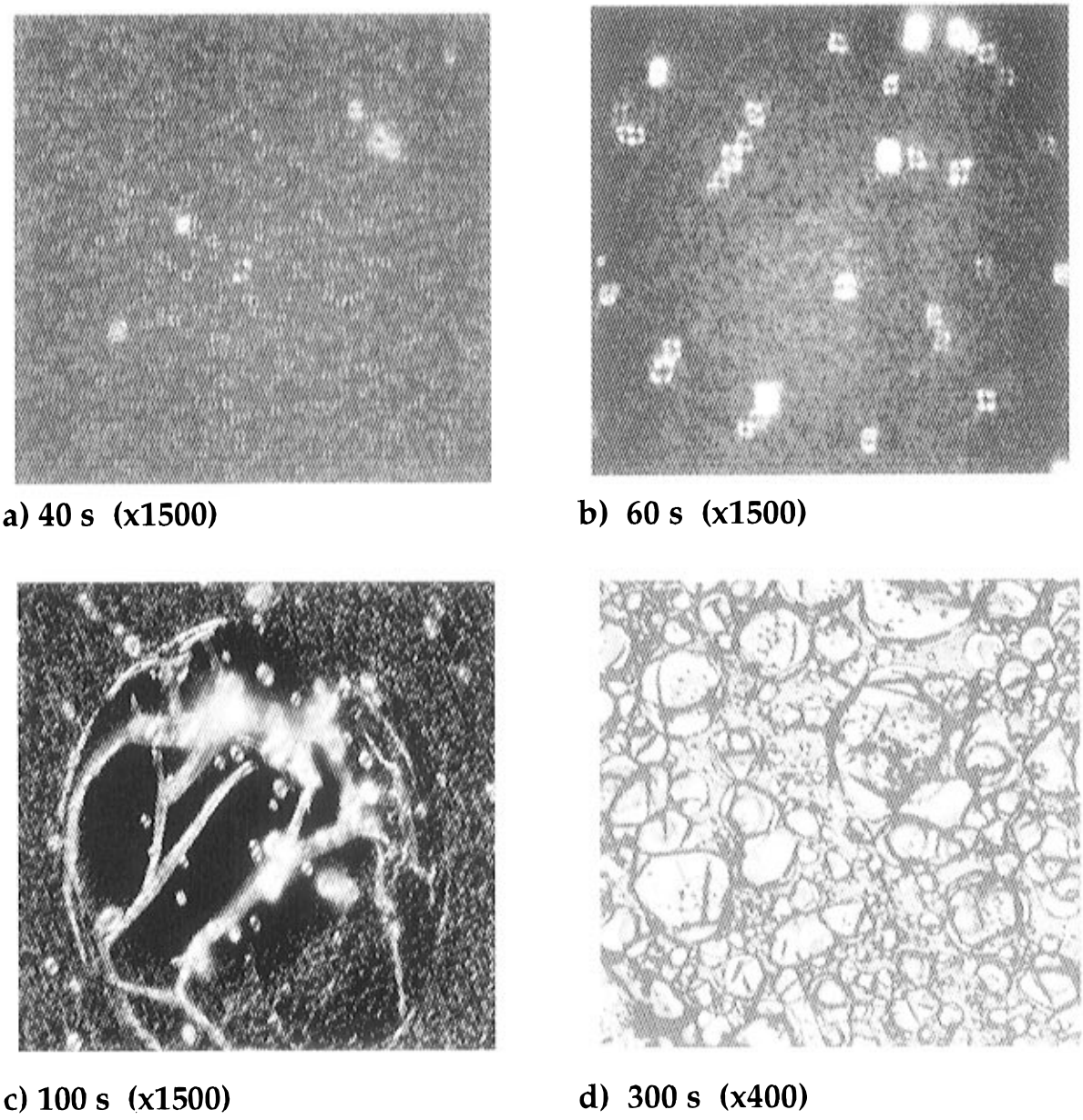

Figure 5. Micrographs illustrating changes during the formation of PPBQ coating at −1 V = const on a sputtered platinum electrode surface (Pt/Ti,W/glass) after (a) 40 s, (b) 60 s, (c) 100 s, and (d) 300 s of polymerization. The PPBQ was deposited in the solution as described for Figure 1.

well-known ECE, mechanism, where E stands for electrochemical reaction and C stands for the follow-up chemical reaction.[21] Furthermore, the mechanisms of protonation of the $BQ^{\bullet-}$ by water may also involve reversible disproportionation of the $BQ^{\bullet-}$ to benzoquinone and benzoquinone bianion (BQ^{2-}).[27] The follow-up reactions lead to the formation of the small oxidation pre-wave on the second redox peak, as shown in Figure 3. The presence of oxygen in the electrolyte had no major effect on the cyclic voltammograms. Addition of water in excess of 1 vol % to the electrolyte shifted the position of the first redox peak to more anodic values and narrowed the distance between the two reduction peaks.

From the disappearance of the oxidation waves for both intermediates ($BQ^{\bullet-}$ and BQ^{2-}) in the presence of the cyclophosphazene (Figure 1), it can be concluded that both of them are consumed. Comparison of Figure 1 with Figure 3 shows that the reaction of the BQ anions with the phosphazene precursor shifts the first reduction wave to more cathodic potentials and affects the second reduction step as well. With repetitive scans, the waves are drawn out and the peak currents gradually and continually decrease in size. In Figure 1 it is observed that after 30 cycles, the second redox wave almost completely disappears. That indicates the complete blockage of the platinum electrode with the film which is insulating. The other quinones systems (naphthoquinone, anthraquinone, and anthrarufin) also gave rise to reversible cyclic voltammograms in the absence of phosphazene trimer. Upon addition of the $(NPCl_2)_3$, the reversibility of the cyclic voltammograms was gradually lost and formation of a film at the electrode was observed.

When a constant potential of −2.0 or −1.0 V was applied (Figure 4), the sigmoidal transient, which fol-

(27) Chon-Hong Pyun; Su-Moon Park. *J. Electrochem. Soc.* **1985**, *132*, 2426.

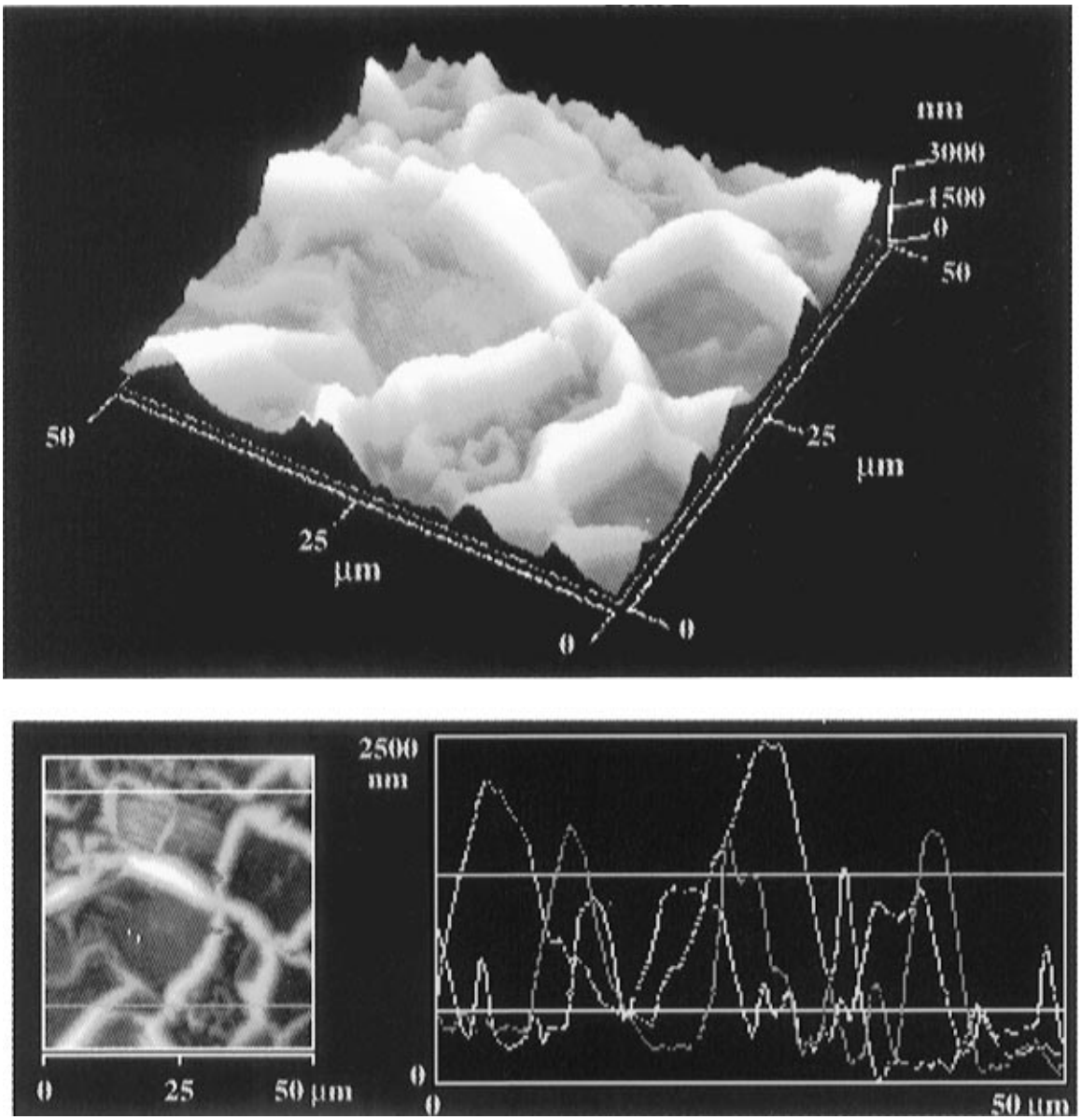

Figure 6. An AFM image of the PPBQ film. The upper picture shows the three-dimensional image of the film. The lower picture shows the down view regions with the selected levels for profilometric thickness measurements. The film was obtained on Au/glass substrate at −1.0 V = const in the solution as described for Figure 1.

lows the $i = f(t^{-1/2})$ decay, confirmed that the polymerization was a diffusion-controlled process. Moreover, the process is essentially controlled by an induction period of 100 s, during which charging of the electrode is taking place. The initial decay of the current is due to a consumption of the electrochemically formed $BQ^{\bullet -}$ and BQ^{2-} species at the electrode surface in a chemical reaction with the electrically neutral $(NPCl_2)_3$ molecules. More detailed information on the nucleation process was obtained by combining electrochemical and optical investigations. In this study the polymerization of PPBQ film was terminated at −1 V after 40, 60, 100, and 300 s, respectively. As shown in Figure 5, after 40 s, the larger nuclei had grown on the platinum surface to an average size of 2 μm (25 pixels in 1500×) (Figure 5a). After 60 s, white agglomerates had progressed to an average size around 3 μm (35 pixels in 1500×) (Figure 5b). After 100 s, the agglomerates had built a type of circular network (Figure 5c) which after 300 s (Figure 5d) developed to a continuous film. The AFM micrograph of the PPBQ film which growth has been terminated after five minutes is shown in Figure 6. The differences between the chemical nature of the two components of the inorganic−organic hybrid coating favor the good intrinsic contrast in the material. The PPBQ is a network-type polymer. The film has a three-dimensional solid-state framework of open rings. The repetition of the trigonal bipyramids governs the cyclomatrix arrangement of the matrix.

Electropolymerization of PPBQ under galvanostatic conditions (5 mA/cm^2) also confirmed that a nucleation process is taking place in the vicinity of the electrode, Figure 7. The high current density guarantees that the electrochemical reaction proceeds at an appreciable rate. The electrochemical irreversibility of the reaction is due to the fast follow-up chemical steps. Consequently, thicker coatings up to 20 μm were deposited by using this mode. This result also implies that the growth of the PPBQ film under potentiostatic conditions is limited by the uncompensated resistance of the coating.

The replacement of the chlorine on the cyclophosphazene trimer is driven by the fact that $BQ^{\bullet -}$ and BQ^{2-}

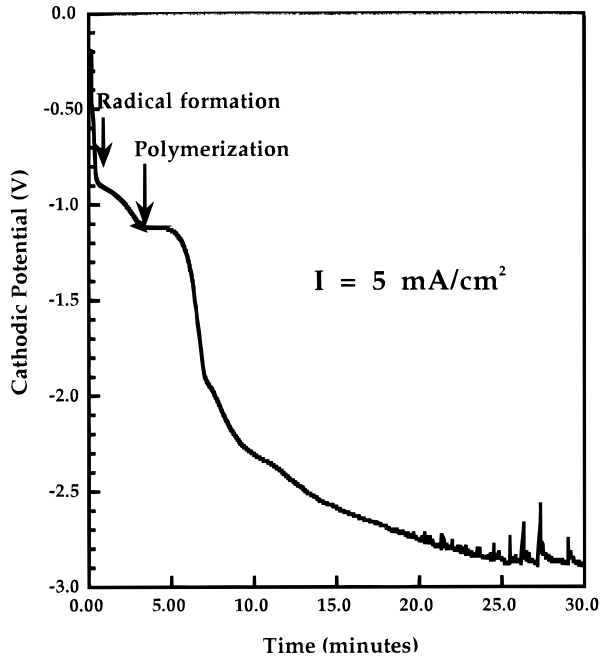

Figure 7. Galvanostatic polymerization of PPBQ at 5 mA/cm^2 in the solution as described for Figure 1.

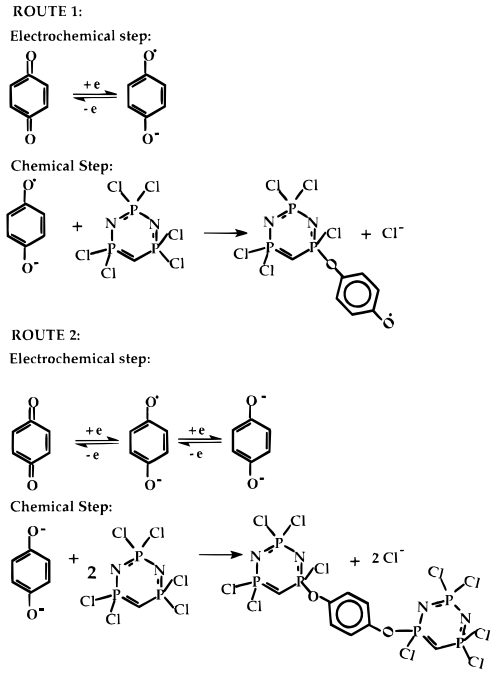

Figure 8. Two proposed electroinitiated polymerization routes of PPBQ films.

are stronger Lewis bases than the chlorine. When the $BQ^{\bullet-}$ displaces the chlorine a formation of the $N_3P_3Cl_5OC_6H_4O^{\bullet-}$ radical as an intermediate takes place, see route 1 (Figure 8). The group $-OC_6H_4O^{\bullet}$ is the reducible group of that intermediate. The reduction takes place at the same potential as for the $BQ^{\bullet-}$ and subsequent nucleophilic substitution of the $N_3P_3Cl_5OC_6H_4O^{\bullet-}$ with another $(PNCl_2)_3$ is taking place. The new intermediate thus formed is electrochemically inactive. The propagation of the polymer chain therefore requires another $BQ^{\bullet-}$. The presence of $(NPCl_2)_3$ in the electrolyte causes a shift in the reduction peak for BQ, from approximately -0.95 to -1.05 V after 20−30 repetitive scans.[10] The reduction of the BQ is fast[27] and the ECEC.. mechanism is therefore controlled only by the kinetics of chemical step.

By setting the cathodic potential $E_{pc2} \geqslant -1.495$ V in the presence of $(NPCl_2)_3$ the EC reaction sequence follows the route 2 (Figure 8). In the chemical step, two of the $(PNCl_2)_3$ trimers are linked by only one BQ^{2-} intermediate. That explains why the growth of the PPBQ films at -2 V is faster than at -1.0 V.

The polymerization process is controlled by the rate constant of the electrochemical/chemical reactions and not by the concentration of the BQ in the solution. Therefore, the polymerization is terminated either by the blockage of the electrode surface by the polymer or by the IR drop in the film which limits the possibility of generation of the $BQ^{\bullet-}$ and BQ^{2-} species. Gas evolution at the cathode leads to formation of cracks in the coating.

The Cl replacement during the nucleophilic substitution of the phosphazene trimer can take place preferentially at the phosphorus by replacing one chlorine atom (geminal replacement) or at phosphorus by replacing two chlorine atoms (nongeminal replacement).[28] For strong nucleophiles such as $BQ^{\bullet-}$ and BQ^{2-}, the electron supply from the exocyclic oxygen should promote replacement of the second Cl on that phosphorus atom, but steric hindrance can also account for the nongeminal mechanism. If the cyclophosphazene precursor has more than two reactive sites, the linkage reaction will generate a three-dimensional structure rather than a linear chain.

The involvement of the $BQ^{\bullet-}$ and BQ^{2-} and the intermediate species such as $N_3P_3Cl_5OC_6H_4O^{\bullet-}$ in π-electron interactions with the $(NPCl_2)_3$ during the polymerization of PPBQ has been also examined spectrophotometrically. In the UV/vis spectra of the catholyte recorded before the PPBQ growth and 10 min after the PPBQ deposition at the platinum electrode at constant potential of -1.0 or -2.0 V, respectively, only the absorption band of the remaining BQ at 242 nm in the electrolyte was detectable, Figure 9a. The absorption maximum of the $(NPCl_2)_3$ which is at 175 nm[29] was outside the UV/vis range used in our experiments. The remaining concentration of BQ depends on the magnitude of the applied potential. Since the lifetime of the $BQ^{\bullet-}$ in acetonitrile solution is approximately 2 h[30,31] a qualitative evaluation of its consumption was also approached. The ratio of $(A_X) - (A_O)/(A_O)$ defined as "normalized absorption" was used as an alternative way to evaluate the effect of the magnitude of the applied cathodic potential of X = -1 V or X = -2 V. The absorbance of the solution recorded before the PPBQ deposition (A_O) was used as a reference. In Figure 9b, two absorbance bands for $BQ^{\bullet-}$ at 417 and 444 nm are identified.[28,30] The relative absorption intensity of the two $BQ^{\bullet-}$ peaks at 417 and 444 nm is lower when -2 V = constant was applied during polymerization. Furthermore, development of an additional weak band at 560 nm, which grows at the expense of the shoulder around 400 nm, is more notable. The narrow absorption band around 280 nm was assigned in the literature to

(28) Allcock H. R. *Chem. Eng. News* **1968**, *46*, 68.
(29) Allcock, H. R. *Phosphorus−Nitrogen Compounds*; Academic Press: New York, 1972; pp 59−64.
(30) Fukuzumi, S. I.; Ono, Y.; Keii, T. *Bull. Chem. Chem. Soc. Jpn.* **1973**, *46*, 3353.
(31) Bauscher, M.; Mäntele, W. *J. Phys. Chem.* **1992**, *96*, 11101.

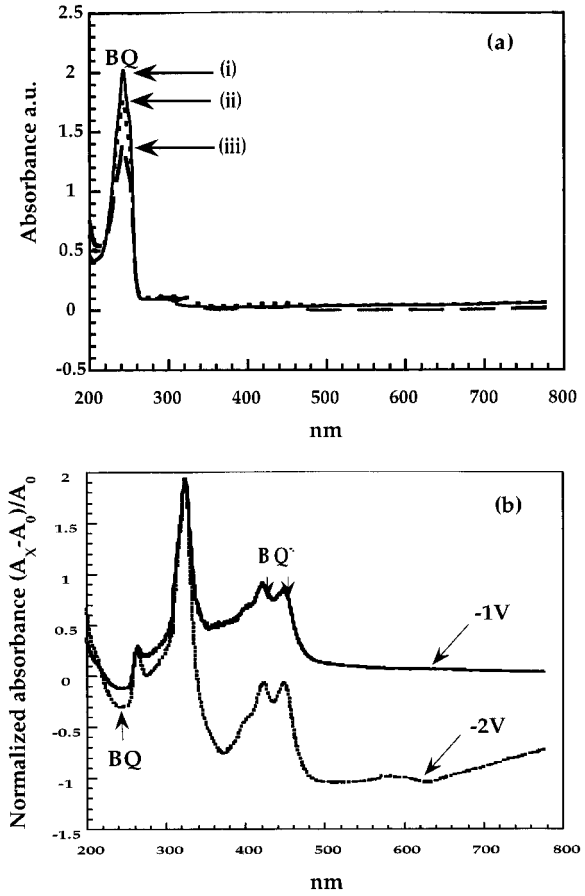

Figure 9. (a) UV/vis spectra obtained after electrolysis carried out from the solution as described for Figure 1. The spectra of the solutions were recorded after dilution 1:20 by volume with acetonitrile (i) before electrolysis and (ii) after 30 min of electrolysis at −1 V= const or (iii) after 30 min of electrolysis at −2 V = const. (b) Normalized UV/vis spectra as shown in (a).

the quinhydrone anion, as the radical anions are protonated.[28]

Characterization of the PPBQ. *Elemental Analysis.* The atomic compositions of two PPBQ films that were synthesized at constant potential of −2 V in the presence of Bu_4NBF_4 or Bu_4NI, are shown in Table 2. The results were independent of the selected mode of deposition. Phosphorus and nitrogen atoms were used as elemental "markers" for the inorganic and organic components. By building the normalized atomic ratio of element A to phosphorus (A/P) we could compare the composition of the synthesized material to the theoretical composition. The discrepancy between the analytical data and the theoretical data can be explained by the presence of the residual salt used as the electrolyte during the synthesis. Analysis of the final carbon and hydrogen content in the polymer demonstrates that the contamination depends on the nature of the electrolyte salt used.

Photoelectron Spectroscopy. To examine the contamination issue of the polymer by the electrolytic salts, we performed surface analyses of the PPBQ film on Pt electrodes by XPS. The sensitivity factors for the elements shown in Table 3 are those of Briggs and Seah.[32] Table 3 shows that C/P increases with the molecular size of the anion chosen as the electrolyte salt. Salt with larger anion size (e.g., BPh_4^- , BF_4^-) adheres more strongly to the coating than salt with the smaller anion (e.g., I^-). Consequently, the ratio of O/P values is also higher with Bu_4NBPh_4 than, for example, with Bu_4NBF_4. The presence of oxygen atoms attached to the phosphorus allows us to determine the number of aryloxy groups substituted for the chlorine atoms. The experimental ratio O/P as compared with the theoretical one equals 1.4. That let us assume that four chlorine atoms have been replaced by four units containing benzenoid groups. Accordingly, with this assumption a chemical structure shown in Figure 10 is proposed. As seen in Table 2, the ratios of C/P and H/P obtained from elemental analysis are higher than those theoretically predicted but the N/P ratio are the same. The Cl/P values were always higher than those determined by the elemental analysis. This result suggests that the surface of the film is terminated by PPBQ molecules containing nonreacted Cl atoms.

FTIR Measurements. To confirm the validity of the proposed structure it was necessary to assign the vibrational frequencies which relate to the phosphazene trimer, hydroquinone, and the -P−O-, P−Cl bonds. Cyclophosphazene compounds show characteristic vibrations in two regions: (i) from 1150 to 1450 cm^{-1} which corresponds to the P−N−P asymmetric ring stretching mode (or degenerate ring stretching mode) and (ii) from 700 to 950 cm^{-1} which corresponds to the P−N−P symmetric stretch. In Figure 11, the KBr FTIR spectrum of the $(NPCl_2)_3$ precursor with its most intense IR absorption at 1208 cm^{-1} is shown. This peak corresponds to the P−N stretching.[33] The absorption peak at 861 cm^{-1} is assumed to correspond to the symmetrical P−N−P stretch.[29] In Figure 12, a and b, the multiple ATR-FTIR spectra of the PPBQ films obtained at constant potentials of −1 or −2 V are shown. First, in both spectra a new IR absorption band around 1500 cm^{-1} is observed. This frequency can be considered as the C−O vibration in the $O-C_6H_4-O$ unit.[30] Its appearance correlates with the change of the benzoquinone structure to the hydroquinone type which is built into the PPBQ polymer chain ($-OC_6H_4O-$). The identification of the new peak at 1500 cm^{-1} was also confirmed by us by recording a KBr FTIR spectrum of a hydroquinone compound not shown here.[12] The P−N stretching vibration mode falls in all spectra around the same vibrational frequency of 1200 cm^{-1} which confirms that the phosphazene ring has been preserved and that the environment around the nitrogen has not been changed. In general, strengthening of a bond should cause an absorption peak to shift to a lower vibrational frequency and weakening of a bond should lead to a shift to higher frequency. The domination of the absorption peak at 1150 cm^{-1} (Figure 12a) or 1162 cm^{-1} (Figure 12b) as compared with 1208 cm^{-1} (Figure 11) indicates that the $-OC_6H_4O-$ group is less electrophilic than Cl and that the skeletal bond-strengthening effect occurs. A possibility exists that the p orbitals of the exocyclic oxygen with the d orbitals of the phosphorus form a π bond. Thus, the P−N stretching should occur for the PPBQ material at lower frequencies than in the spectra

(32) Briggs, D.; Seah, M. P. *Practical Surface Analysis*, 2nd. ed.; Wiley: New York, 1990; Vol. 1, p 635.

(33) Niquist, R. A.; Potts, W. J. In *Analytical Chemistry of Phosphorous Compunds*; Halmann, M., Ed.; Wiley-International: New York, 1972; Chapter 5, p 189.

Table 2. Comparison of Atomic Composition of Two PPBQ Films Obtained by Elemental Analysis[a]

	synthesis from Bu4NBF4		synthesis from Bu4NBI		
atom	elem anal (wt %)	atomic ratio A/P[b]	elem anal (wt %)	atomi ratio A/P[b]	theoretical atomic ratio A/P[c]
C	39.46	6.27	33.93	4.4	4.0
H	4.00	7.6	3.44	5.4	2.7
N	7.86	1.07	10.04	1.1	1.0
P	16.27	1.0	19.77	1.0	1.0
Cl	11.33	0.61	15.52	0.68	0.68
F	4.62	0.46			
I			< 0.5		

[a] The films were deposited from 0.01 M $(NPCl_2)_3$ and 0.01 M BQ in acetonitrile, in the presence of two electrolytes. [b] Calculation of A/P atomic ratio is based on the elemental analysis data. [c]Calculation of A/P is based on the proposed molecular formula of one PPBQ polymer unit shown in Figure 10.

Table 3. Comparison of Atomic Compositions of PPBQ Films Obtained from XPS Experiments[a]

	PPBQ synthesized in the presence of			
	N/P	C/P	Cl/P	O/P
0.1 M Bu_4NI	1.06	4.31	0.96	1.44
0.1 M Bu_4NBF_4	1.08	6.12	0.92	1.40
0.1 M Bu_4NBPh_4[b]	1.06	7.71	1.06	2.14

[a] The atomic ratios of the elements have been normalized to phosphorus. The films were deposited from 0.01 M $(NPCl_2)_3$ and 0.01 M BQ in acetonitrile in the presence of three electrolytes. [b] Bu_4NBPh_4 stands for tetrabutylammonium tetraphenylborate.

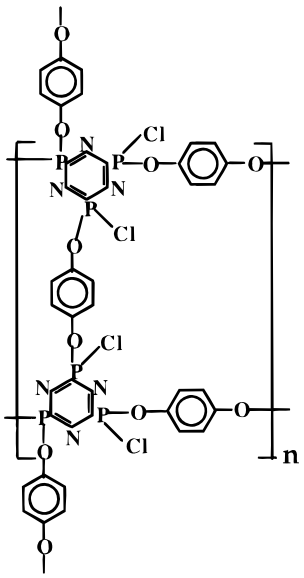

Figure 10. Proposed molecular structure of one unit of the PPBQ film.

of the phosphazene monomer. Analogously, the P−N vibrations associated with the symmetric N−P−N stretching are shifted to higher frequency from 861 to 875 cm^{-1} for the PPBQ polymer as compared with the $(PNCl_2)_3$ precursor. It appears that the symmetric ring stretches are much less sensitive to the P−N−P bond polarization than the asymmetric stretches. The appearance of the peaks at the 962 and 837 cm^{-1} (Figure 12a) and at 954 and 838 cm^{-1} (Figure 12b) results from the coupling of the $BQ^{\bullet-}$ to the N−P bond through the P−O bond.

^{31}P NMR Measurements. Interpretation of the ^{31}P NMR chemical shifts for cyclophosphazenes are difficult. Substituent effects on phosphorus chemical shifts will depend on a complex interplay of electronegativity, bond angles, and the changes in occupancy of phosphorus p and d orbitals.[34] Positive shifts are associated with greater shielding of the phosphorus.[30] Keat has reported a chemical shift for $(PNCl_2)_3$ at 19.3 ppm from the liquid ^{31}P NMR.[35]

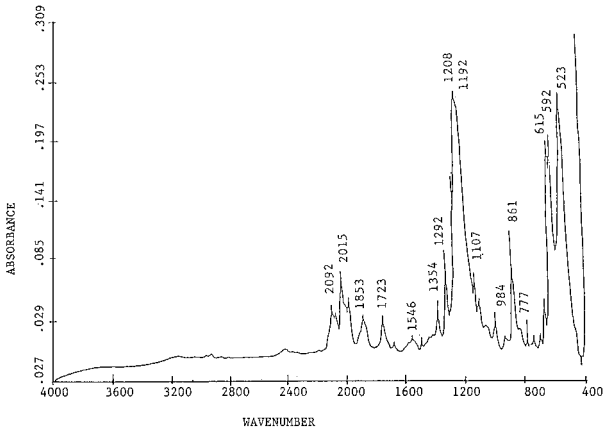

Figure 11. FTIR spectrum of $(NPCl_2)_3$ powder with KBr (see the text for peak assignments).

The solid state ^{31}P NMR spectra obtained on $(PNCl_2)_3$ and on PPBQ coatings are shown in Figure 13. In the solid ^{31}P NMR we determined for the phosphorus the chemical shift in $(PNCl_2)_3$ at the middle peak at 19.7 ppm. The chemical shift at 3.8 ppm is due to the hydration of $(PNCl_2)_3$ in air. The chemical shifts for the PPBQ film are 24.1 and 7.5 ppm. They signal two different environments of the phosphorus. Their positive chemical shifts confirm that the ring structure is maintained in the polymer.[30] Positive chemical shift of phosphorus to 7.5 ppm indicates a greater nuclear shielding in the compound under investigation relative to the reference compound, $(PNCl_2)_3$. Assuming that chlorine is replaced by the less electron-withdrawing $-OC_6H_4O-$ group, the positive charge on the phosphorus is expected to decrease in magnitude and a positive chemical shift should be observed.[36, 37] That may provide an evidence for the delocalization of the π-orbital. It was observed by others that the chemical shifts of the P(Cl)(OPh) and $P(OPh)_2$ in $P_3N_3Cl(OPh)_5$ are 22.1 and 6.9 ppm, respectively.[38,39] Assuming that a rough correlation between the peak shift obtained for PPBQ polymer and the literature data exists, analogous as-

(34) Krishnamurthy, S. S.; Woods, M. *Annu. Rep. NMR Spectrosc.* **1987**, *19*, 175.
(35) Keat, R.; Shaw R. A.; Woods, M. *J. Chem. Soc., Dalton. Trans.* **1976**, 1583.
(36) Dake, L. S.; Baer, D. R.; Ferris, K. F.; Fredrich, D. M. *J. Electron Spectrosc. Relat. Phenom.* **1990**, *51*, 439.
(37) Branton, G. R.; Brion, C. E.; Frost, D. C.; Mitchell, A. R.; Paddock, N. L. *J. Chem. Soc. A.* **1970**, 151.
(38) Allcock, H. R.; Evans, T. L.; Fuller, T. J. *Inorg. Chem.* **1980**, *19*, 1026.
(39) Telkova, I. B; Korshak, V. V.; Volodin, A. A.; Fomin, A. A. *Zh. Obshch. Khim.* **1973**, *43*, 1257.

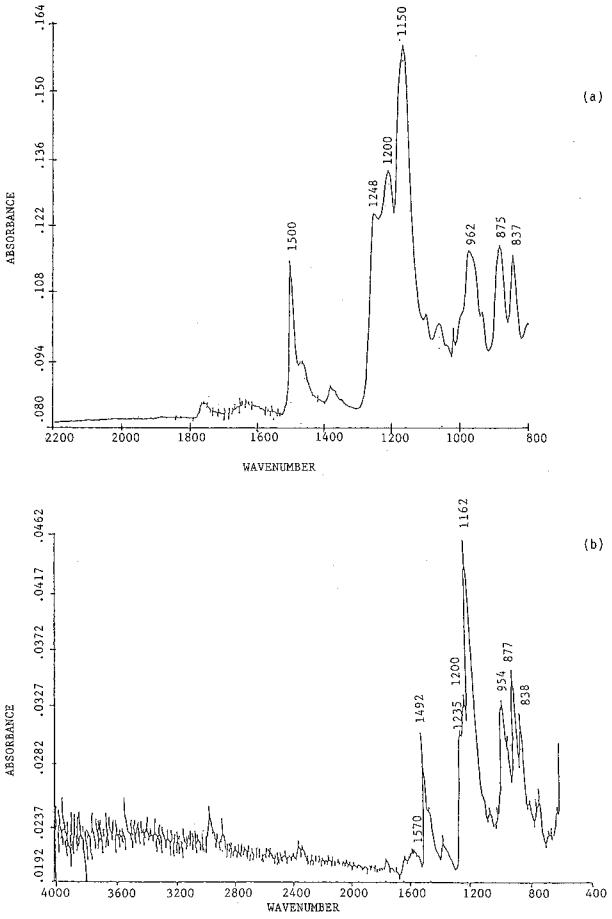

Figure 12. ATR-FTIR spectra of PPBQ films deposited (a) at −1 V = const for 5 min and (b) at −2 V = const for 5 min.

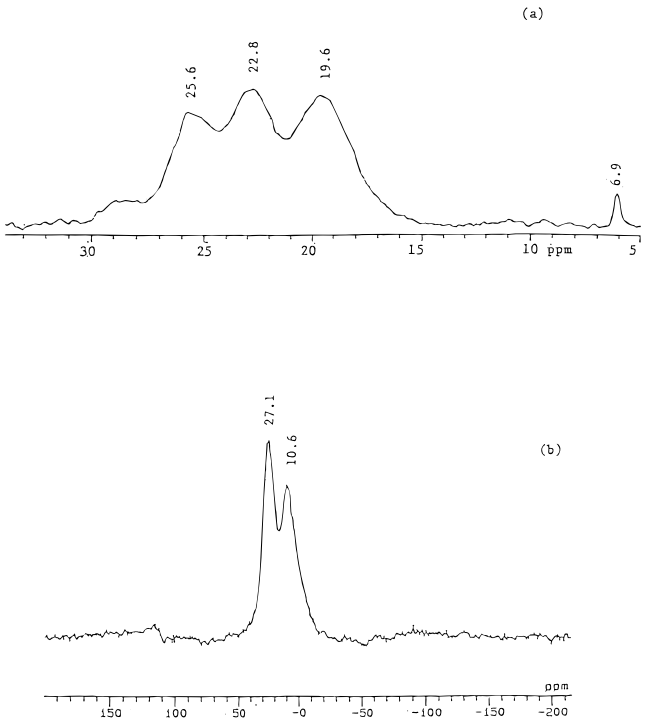

Figure 13. ^{31}P NMR spectra of $(PNCl_2)_3$ precursor (a) and PPBQ film (b). The measured chemical shifts are presented versus the reference $(C_6H_5O)_3P$ at $\delta = -3.1$ ppm.

signments for the chemical shift of the polymer at 24.1 ppm to P(Cl)(OPhO) and at 7.5 ppm to $P(OPhO)_2$ is proposed. The discrepancies in the peak positions for the polymer and the $P_3N_3Cl(OPh)_5$ compound indicate

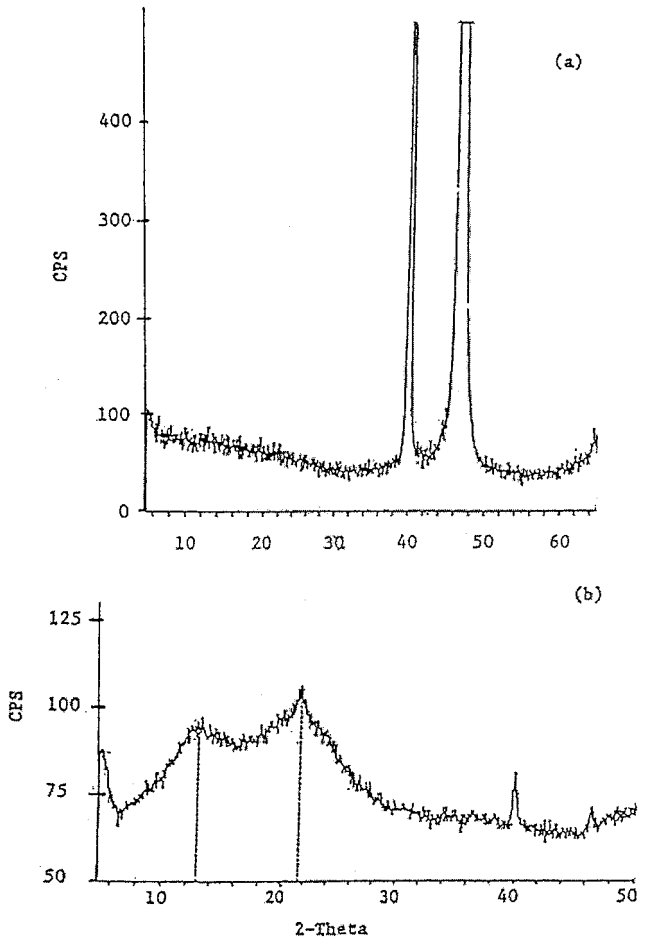

Figure 14. X-ray diffraction patterns of PPBQ (a) deposited on Pt foil at −1.0 V and (b) powder (3.21 mg) which was obtained by scratching off the polymer from the Pt foil substrate.

that structural differences (due to differences and alternation of bonding angles) may cause the chemical shifts to 24.1 ppm from 22.1 and 7.5 ppm from 6.9 ppm, respectively. Since the chemical shift of the PCl_2 unit at 19.7 ppm did not show up in the PPBQ spectrum, it is apparent that at least one of the two chlorine atoms on the phosphorus was substituted by $-OC_6H_4O-$ unit.

X-ray Diffraction. Figure 14a shows the X-ray diffraction patterns of the powdered PPBQ coating obtained on a platinum substrate. The two sharp features at the diffraction angle, 2θ, equal to 39.5° and 46° correspond to metallic platinum. Figure 14b shows the XRD patterns of the powdered coatings. The inspection of the XRD data for a cyclic trimer, which is highly crystalline,[40,41] permits us to conclude that the PPBQ material is amorphous. The two broad bands at 2θ equal to 12.8° and 21.5° have considerable three-dimensional disorder.

Electrochemical Results. The electrochemical activity of the PPBQ coating on Pt electrode was examined by comparing the cyclic voltammograms with uncoated Pt electrode (Figure 15). The drop in the current magnitude as well as the change of the shape of the cyclic voltamograms from sigmoidal to limiting curren, signalizes that the deposited PPBQ coating is not electrically

(40) Bullen, G. J. *J. Chem. Soc. A* **1971**, 1450.
(41) deSantis, P.; Giglio, E.; Ripamonti, A. *J. Inorg. Nucl. Chem.* **1962**, *24*, 469.

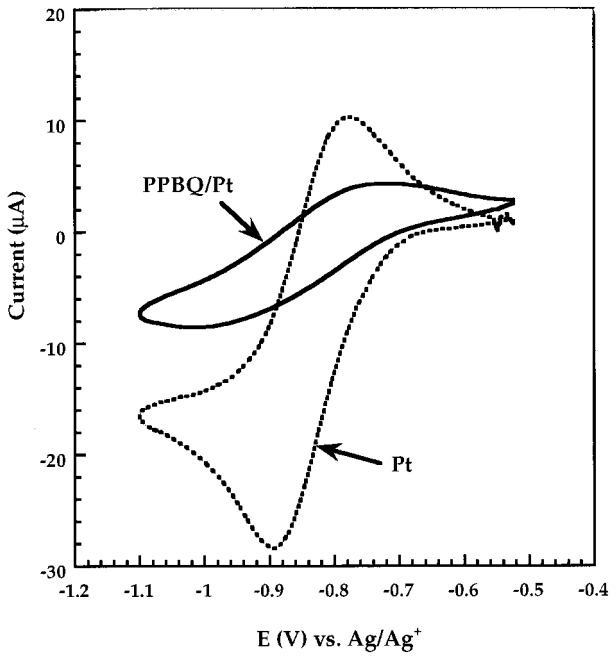

Figure 15. Comparison of cyclic voltammograms of the BQ/$BQ^{\bullet-}$ redox couple recorded in the presence of 2 mM BQ, 0.1 M Bu_4NBF_4 in acetonitrile for platinum electrode (Pt), and PPBQ-coated platinum eleclectrode (PPBQ/Pt) with the scan rate of 100 mV/s.

conducting and it is porous. Cyclic voltammograms obtained on the PPBQ-modified electrode in a solution containing redox couples such as $Ru(NH_3)_6^{2+}/Ru(NH_3)_6^{3+}$ and $Fe(CN)_6^{2+}$ /$Fe(CN)_6^{3+}$, which are not shown here, clearly identify that the porosity of the film is controlled by the applied potential during the synthesis. Films deposited at −1 V are less permeable to the redox ions than the films deposited at −2 V.[12]

Finally, the chemical resistance of the coating to strong acids (nitric acid, sulfuric acid, hydrochloric acid), strong base (sodium hydroxide, ammonium hydroxide), and strong oxidant (ammonium persulfate and hydrogen peroxide) as well as organic solvents (tetrahyfrofuran, toluene, benzene, chloroform, propylene carbonate) has been examined. The PPBQ coatings resist exposure to those chemicals. To destroy the coating we found out that it is necessary to apply to the PPBQ-modified electrode a constant potential of +4 V in 4.5 M H_2SO_4 solution for approximately 10 h. Under these extreme oxidation conditions the coating cracks and finally peals down. The PPBQ also does not melt but sublimes at temperatures higher than 240 °C and is not flammable. The density of the coatings is about 1.2 g/cm^3.

Summary

The potentiostatic and spectrophotometric experiments provide strong evidence that the reduction of the BQ in the presence of Bu_4NBF_4 in acetonitrile at the cathode is a two-step reversible process leading to formation of strongly basic $BQ^{\bullet-}$ and BQ^{2-} as intermediates (eq 1 and eq 2). These in situ generated intermediates at the electrode surface attack the P−Cl bond of the $(PNCl_2)_3$ and form the PPBQ film under controlled ECEC.. mechanism. The magnitude of the applied cathodic potential affects the growth of the polymer but not the composition of the deposited material. The texture of the coating varies with the selected mode of deposition; films deposited using potentiostatic technique differ from those deposited using galvanostatic technique. Because PPBQ is deposited cathodically it can be grown on variety of electrode materials.

FTIR and ^{31}P NMR spectroscopy experiments have provided useful information about the micromolecular structure of the PPBQ material. The observed peak vibration frequency at 1200 cm^{-1} confirmed that the asymmetric ring stretching of the P−N−P of the phosphazene ring remains intact. The positive chemical shifts in ^{31}P NMR spectra ascertain the identity of the maintained ring structure of the phosphazene trimer. Furthermore, two different phosphorus environments due to the presence of $P-(OC_6H_4O)_2$ and $P-(-OC_6H_4O)$-(Cl) bonds in the polymer were identified. The presence of the $P-OC_6H_4O$ bond and the P−Cl bond was also recognized in the recorded ATR−-FTIR spectra. X-ray diffraction experiment shows that this material is not crystalline. From the elemental analysis and XPS experiments it was calculated that four of the chlorine atoms of the $(PNCl_2)_3$ precursor have been replaced by four aromatic groups. The AFM micrographs confirmed a three-dimensional macromolecular arrangement in the film. The PPBQ acts as an electrically insulating barrier because the aromatic units are separated from the phosphazene ring by an exocyclic oxygen. The coating is porous and its porosity can be controlled by electrochemical deposition mode.

Acknowledgment. This research was supported by the DOE/N-20 Program. The authors are indebted to Li-Qiong Wang, David McQuerry, Mark Engelhard, and Glen Dunham for their assistance in NMR, X-ray difraction measurements, XPS measurements, and quartz crystal microbalance. Special thanks to Jiří Janata, Gregory J. Exarhos, Don R. Baer, and William D. Samuels for valuable discussions.

CM9701365